

Damping filter method for obtaining spatially localized exact solutions

Toshiki Teramura* and Sadayoshi Toh

Department of Physics and Astronomy, Graduate School of Science, Kyoto University, Japan

(Dated: November 24, 2021)

Spatially localized structures are key components of turbulence and other spatio-temporally chaotic systems. From a dynamical systems viewpoint, it is desirable to obtain corresponding exact solutions, though their existence is not guaranteed. A damping filter method is introduced to obtain variously localized solutions, and adopted into two typical cases. This method introduces a spatially selective damping effect to make a good guess at the exact solution, and we can obtain an exact solution through a continuation with the damping amplitude. First target is a steady solution to Swift-Hohenberg equation, which is a representative of bi-stable systems in which localized solutions coexist, and a model for span-wisely localized cases. Not only solutions belonging to the well-known snaking branches but also those belonging to an isolated branch known as “isolas” are found with a continuation paths between them in phase space extended with the damping amplitude. This indicates that this spatially selective excitation mechanism has an advantage in searching spatially localized solutions. Second target is a spatially localized traveling-wave solution to Kuramoto-Sivashinsky equation, which is a model for stream-wisely localized cases. Since the spatially selective damping effect breaks Galilean and translational invariances, the propagation velocity cannot be determined uniquely while the damping is active, and a singularity arises when these invariances are recovered. We demonstrate that this singularity can be avoided by imposing a simple condition, and a localized traveling-wave solution is obtained with a specific propagation speed.

PACS numbers: 47.27.ed, 47.10.Fg, 47.27.nd

I. INTRODUCTION

A dynamical systems point of view and accompanying exact solutions to Navier-Stokes equation play key roles in understanding the dynamics of turbulence [1]. It is useful both in transient flows and statistically steady flows. Indeed in minimal turbulence [2], a crucial aspect of the dynamics of laminar-turbulent transition processes has been revealed by the discovery of “edge state” [3, 4], and that of the self-sustaining process (SSP) has been done by the discovery of unstable periodic orbits which reproduce the statistics of turbulence [5].

The dynamical systems viewpoint, however, has not yet successfully captured the full nonlinear spatio-temporal dynamics of turbulence. One major limitation is that there is no general framework for obtaining solutions corresponding to spatially localized structures in turbulence. For example, in channel flows there exist near-wall structures and large scale motion (LSM) that occupies the outer layer above the near-wall layer. In order to elucidate their intrinsic dynamics and interactions among them from the dynamical systems viewpoint, it is desirable to obtain corresponding exact solutions separately. Such localized exact solutions are paid much attention recent years, and indeed obtained in a few cases [6–9]. However, despite of their importance, any practical ways to obtain them have not established yet. For this purpose, we introduce a damping filter method in Section II.

There exist various types of localized structures. For example, turbulent puffs in pipe flow are localized in the stream-wise direction; turbulent spots in channel flow do both in the stream-wise and span-wise directions. If there exists a solution corresponding to LSM, it will be localized in the wall-normal direction. In this paper, we focus on the two typical cases both of which will be instructive in understanding localized structures observed in turbulence. We show not only basic usage and results but also remarkable features of our method in Sections III and IV.

We first consider localized solutions to Swift-Hohenberg equation (SHE) [10–12]. This is a representative example of localized solutions in bi-stable systems. This class of localized solutions contains, for example, span-wisely localized solutions corresponding to roll-streak structures in plane Couette flow [13]. Their solution branches are very similar to the “snaking” branches seen in SHE [10]. Similar structures of solution branches are also found in doubly diffusive convection systems [14]. These facts indicate that there exists a universal mechanism of spatially localized solutions in the bi-stable systems. We deal with solutions in this class in Section III.

Second, we examine a spatially localized traveling-wave solution to Kuramoto-Sivashinsky equation. Such a solution can be regarded as a stream-wisely localized solution. Stream-wisely localized structures can be observed in pipe flow (turbulent puffs), boundary layers (hairpin vortices), and so on. The sustaining mechanism of them might be different from that of span-wisely localized solutions, and thus it is necessary to obtain the corresponding solutions in order to analyze them from a dynamical systems viewpoint. At a glance, since our method utilizes a spatially selective damping effect that

* teramura@kyoryu.scphys.kyoto-u.ac.jp

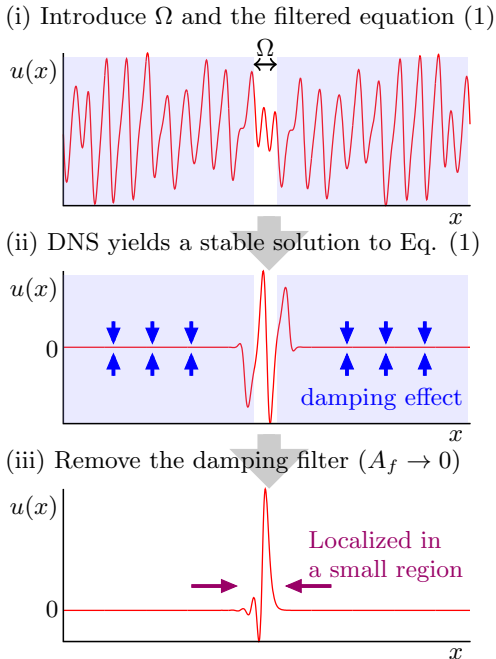


FIG. 1. (Color online) Three steps in the damping filtering method.

breaks translational invariance, it seems to have only limited capability for this issue. However, we show that this is not the case in Section IV.

This paper is organized as follows. In Section II, a damping filter method is introduced, where we explain its concept and concrete procedure. In Sections III and IV we adopt the method to Swift-Hohenberg equation and Kuramoto-Sivashinsky equation respectively in order to obtain spatially localized solutions. Finally, this paper is concluded with concluding remarks in Section V.

II. DAMPING FILTER METHOD

In this section the protocol of the damping filter method is explained. This method consists of three steps. Since this method can be used for various systems, a general form evolution equation, $\partial_t u = F[u]$, is used in the following explanation.

The first step of this method is to introduce a spatially selective damping term into the evolution equation. The damping term works only in a region Ω . If we want to obtain a span-wisely localized solution, Ω should be a region localized in span-wise direction. If we want to obtain a solution localized like turbulent spot, Ω should be a spot region. Then the damping term is introduced as follows:

$$\partial_t u(x, t) = F[u](x, t) - A_f H(x)u(x, t). \quad (1)$$

We call this equation “filtered equation” hereafter. The damping term consists of the filter amplitude A_f and a filter function $H(x)$. $H(x)$ is defined to be zero in the

region Ω and to be 1 out of Ω , and smoothed by taking a convolution with a mean-zero Gaussian $\mathcal{N}_{0, \sigma^2}(x)$ in order to avoid the numerical singularity:

$$H(x) = \int \mathcal{N}_{0, \sigma^2}(x - y) \hat{H}(y) dy, \quad (2)$$

$$\hat{H}(x) = \begin{cases} 0 & (x \in \Omega) \\ 1 & (x \notin \Omega) \end{cases}. \quad (3)$$

The integral is taken in the whole region. The damping term causes a linear damping effect out of Ω (filtered region), and the filtered equation equals to the original equation $\partial_t u = F[u]$ in Ω (unfiltered region).

The second step is to obtain an exact solution to the filtered equation (1). Owing to the spatially selective damping effect, the direct numerical simulation (DNS) of the filtered equation tends to yield a spatially localized time series $u(x, t)$, in other words, $u(x, t)$ decreases exponentially fast as x goes away from Ω after a relaxation time. In addition, since the damping effect weakens the instability of the system, DNS sometimes yields a non-trivial stable solution for enough large filter amplitudes and an appropriate Ω . In this case the second step is finished with this stable solution. If any stable solutions are not obtained, a solution to the filtered equation is obtained by solving an equation $F[u] - A_f H(x)u = 0$ about $u(x)$ with Newton method. Since the degree of freedom is also reduced by the damping term, it is expected that such a solution can be obtained easily.

The third step is a continuation process. The solution obtained in the second step depends on the filter amplitude A_f , and often this dependency is continuous. A continuation with A_f is started from this solution. The filter amplitude A_f is decreased until it gets to zero, where the filtered equation is restored to the original equation in the whole region. Then the continued solution is nothing but that to the original equation. This is the goal of the damping filter method. The continuation is implemented by the arc-length method with Newton-Krylov iterative method, and thus applicable to systems having large degree of freedom.

The good feature of our method is that an appropriate guess of a spatially localized solution is constructed as a solution to the filtered equation (1). This guess reflects the dynamics of spatially localized structures since the filtered equation equals to the original equation in the region Ω . In another study [15], an artificial external forcing is used for constructing a guess of solutions. It was designed by hand from the inference about the dynamics of localized structures. In our method such artificial manipulation is not needed except for determining the region Ω .

This spatially selective damping is inspired by the work [16]. They have investigated an autonomous behaviors of near-wall structures by a filtered dynamics. In contrast to them, our method uses this filtered dynamics only for guesses and continuations, and removes the filter finally. Thus, our method enable us to study the non-filtered dynamics by localized solutions.

III. SPAN-WISELY LOCALIZED SOLUTIONS

In this section we consider one-dimensional Swift-Hohenberg equation (SHE):

$$\frac{\partial u}{\partial t} = F[u] = \left(r - \left(\frac{\partial^2}{\partial x^2} + 1 \right)^2 \right) u + 2u^3 - u^5. \quad (4)$$

As noted in the introduction, a series of solutions to SHE is regarded as a representative of localized solutions in the bi-stable systems. The following subsections show two things: (i) We can obtain span-wisely localized solutions by our method. In order to show this, we reproduce solutions belonging to the homoclinic snaking branches. The practical detail of our method is also described. (ii) Our method has a capability for obtaining various solutions that are usually hard to be found. Indeed, we find an isolated and closed solution branch. Since isolated solution branches cannot be found by the weakly nonlinear framework, this success indicates an advantage of our method.

A. Homoclinic snaking branches

In this subsection we apply our method to SHE in order to obtain a localized steady solution belonging to the snaking branches. Although the branches contain stable localized solutions for a parameter region, the attracting basins of them are very small, and thus it is almost impossible to obtain these localized solutions by DNSs with arbitrary initial conditions.

Before adopting our method, the setting of system is described. We consider SHE in a region $[0, L]$, $L = 180$, and impose a fixed boundary conditions $u(0) = u(L) = 0$. The parameter r is set to -0.669 in this subsection, and -0.633 is used in the next subsection. Time evolutions are solved by the quasi-spectral method with the classical fourth-order Runge-Kutta method. We regard a steady point of DNS as a steady solution to the equation, so the DNS code is used also in continuation processes.

We describe the practical details of our method hereafter. The first step of our method is to introduce the damping term. The unfiltered region Ω is set to be $[80, 100]$, and the filter function $H(x)$ is smoothed with $\sigma^2 = 0.01$. The amplitude of the filter A_f is set to be 1.

The second step is to obtain an solution to the filtered equation (1) with $F[u]$ of Eq. (4). This equation has a stable localized steady solution with these parameters. The initial condition of this DNS is the stable steady sine-like solution of non-filtered equation (4), which is not spatially localized but spatially extended. Such a localized solution to the filtered equation exists while $r \lesssim -0.72$. This lower limit almost agrees with that of the snaking branches. Since the spatial period of the sine-like solution is 2π , these localized solutions to the filtered equation contain almost three periodic components.

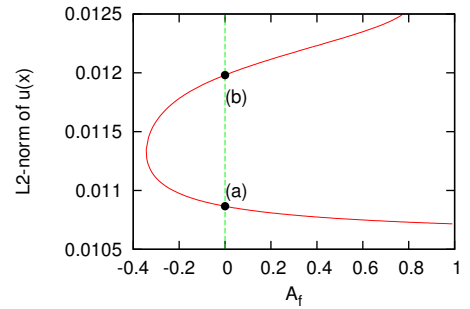


FIG. 2. (Color online) The trajectory of continuation projected onto a A_f - $\|u\|$ space. Each of two labeled solutions (a),(b) on the line $A_f = 0$ denotes a solution to SHE. The continuation is continued after the filter amplitude A_f became zero, and yield a solution labeled (b). The profile of these solutions are shown in Fig. 3.

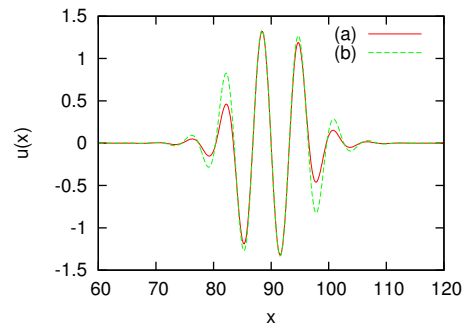


FIG. 3. (Color online) The profiles of the solutions obtained in the continuation shown in Fig. 2. Since the tails of the solutions decay exponentially, These solutions are localized almost in $[70, 110]$, and have an exponentially decaying tail.

The third step is a continuation process. The parameter traced in this continuation is the filter amplitude A_f , and the parameter r is fixed. The result of the continuation is shown in Fig. 2, which displays the trajectory of the continuation projected onto a A_f - $\|u\|$ plane. Here $\|\cdot\|$ denotes the L^2 -norm. The trajectory crosses the line $A_f = 0$ twice. Although a solution to SHE is obtained when the trajectory crosses the line first and thus the damping filter method finishes at this time, we find that the trajectory turns back and crosses the line $A_f = 0$ again. Eventually, we successfully obtain two solutions to SHE, and the profile of them are shown in Fig. 3. These solutions are localized almost in $[70, 110]$, which is larger than $\Omega = [80, 100]$. This fact indicates that Ω is only a guide for obtaining a spatially localized solution, which obeys not the damping filter but the original equation.

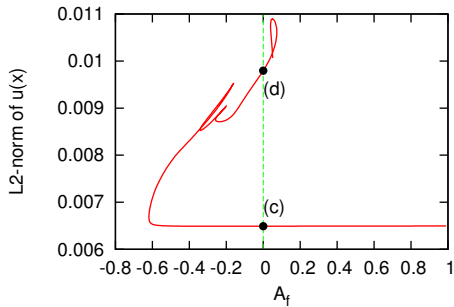


FIG. 4. (Color online) The trajectory of continuation projected onto A_f - $\|u\|$ started from an unstable solution to the filtered equation. This continuation also cross the line $A_f = 0$ twice, but a complicated path is realized. Two labeled points (c) and (d) on the line $A_f = 0$ are also solutions to SHE, and their profiles are shown in Fig. 5. As noted in the text a switching between solution branches are occurred in this complicated part of the trajectory.

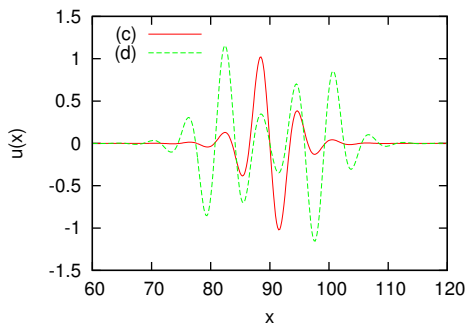


FIG. 5. (Color online) The profiles of the solutions (c) and (d). In contrast to Fig. 3, the profiles of the solutions (c) and (d) are qualitatively different.

B. An isolated closed branch

We execute the same procedure for various values of the parameter r . For most of r it yields continuation trajectories and solutions to SHE similar to those shown in the previous section. However, we also find quite different behaviors in some cases, one of which we focus on in this subsection.

As an initial guess we use a solution to the filtered equation obtained by a continuation with the parameter r started from the solution to the filtered equation used in the previous section. The other parameters are same as those of the previous section: $\Omega = [80, 100]$ and $A_f = 1$.

The result of the continuation with A_f starting from this starting solution is displayed in Fig. 4. Compared with Fig. 2, the continuation trajectory is very complicated especially in the region $A_f < 0$. The two solutions on the line $A_f = 0$ are labeled as (c) and (d), and their profiles are displayed in Fig. 5.

A difference between the solutions (c) and (d) can be observed in its profile: The solution (c) is a single pulse solution like the solutions (a) and (b). On the other

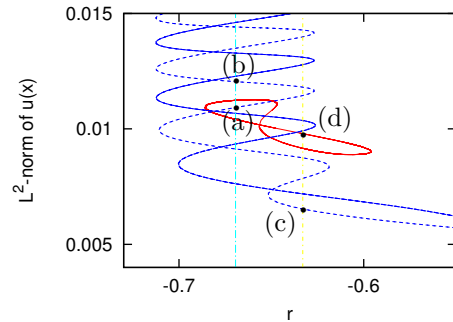


FIG. 6. (Color online) The snaking branches and isolas projected onto a r - $\|u\|$ plane. The snaking branches consist of two coupled branches, and solutions (a), (b) and (c) belong to the same one of them (dashed blue line). The red (dark gray) figure-eight shaped line denotes the isolas containing the solution (d). Such eight-figured branches can be seen also in two-pulse solutions to SHE [17]. This similarity tells that the solution (d) should be regarded as a connected two-pulse solution.

hand, the solution (d) seems to be a combination of two antisymmetric pulse solutions. There exists the definitive difference in their solution branches as shown in Fig. 6. This figure shows that the solutions (a), (b), and (c) belong to the snaking branches, but the solution (d) belongs to an isolated closed branch. Such closed isolated solution branches are called “isolas” in [17].

It should be noted that two distinct branches are connected by the continuation with A_f . Moreover, they connect through the region where A_f becomes negative, where the term $-A_f H(x)u$ works as an excitation term. Thus the connection can be regarded as a result of the instability caused by this term. Since $u(x)$ has an exponentially decaying tail, this instability occurs only around the edge of Ω . So this linear excitation is also spatially selective.

IV. STREAM-WISELY LOCALIZED SOLUTIONS

In this section a stream-wisely localized solution, in other words, a solution localized in its moving direction is studied with Kuramoto-Sivashinsky equation (KSE):

$$\frac{\partial u}{\partial t} = F[u] = -u \frac{\partial u}{\partial x} - \frac{\partial^2 u}{\partial x^2} - \frac{\partial^4 u}{\partial x^4}. \quad (5)$$

It should be noted that KSE has no localized equilibrium solution whose tail decays exponentially. If we adopt our method to Eq. (5), the continuation about A_f yields the flat solution $u = 0$ before A_f reaches zero. So we seek a stream-wisely localized traveling-wave solution (TWS) such that $u(x, t) = \hat{u}_0(x - ct)$ satisfying boundary conditions $\hat{u}_0(x - ct \rightarrow \pm\infty) \rightarrow 0$.

In contrast to the case of span-wisely localized solutions, there are two issues in this case: One is a treatment of the propagation velocity of the solution, and the

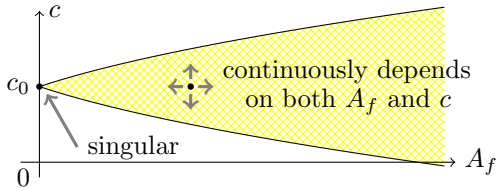


FIG. 7. (Color online) An image for the continuous existence of solutions and singularity at $A_f = 0$. The existence of the solution is displayed in A_f - c plane. The solution exists continuously on the yellow (thin gray) crosshatched region, and cannot be traced beyond its rim. There is no guarantee that this solution branch connects to the line $A_f = 0$. If it does, only a point is allowed because the solution cannot exist continuously on the line $A_f = 0$.

other is a breakdown of the localization. These issues will arise in more general cases since they are based on Galilean and translational invariances. In the following subsections a solution to these issues are described.

A. A treatment of the propagation velocity

Since a TWS travels downstream, its localized region must accompany. In order to obtain a localized TWS by our method, it is necessary to introduce a moving damping filter or a steady damping filter in a moving frame, and we chose the latter. Then the equation becomes as follows:

$$\frac{\partial \hat{u}}{\partial t'} = -(\hat{u} - c) \frac{\partial \hat{u}}{\partial x'} - \frac{\partial^2 \hat{u}}{\partial x'^2} - \frac{\partial^4 \hat{u}}{\partial x'^4} - A_f H(x') \hat{u}, \quad (6)$$

where $x' = x - ct$, $t' = t$, $\hat{u}(x', t') = u(x, t)$. We seek a steady solution satisfying $\partial_{t'} \hat{u} = 0$ in this frame. However, the velocity of the moving frame c is unknown unless the solution is obtained. Since KSE does not allow their solutions to continuously depend on c , a specific value c_0 with which a solution $\hat{u}_0(x - c_0 t)$ exists must be determined simultaneously.

Such a situation sometimes occurs when obtaining a TWS to an equation $\partial_t u = F[u]$. In these cases, this problem is usually resolved by regarding c as an unknown variable, and solving $-c \partial_x u = F[u]$ for $u(x)$ and c . Since the translational invariance reduces the degree of freedom, this simultaneous equation can be solved. In our method, however, the damping filter breaks Galilean and translational invariances, thus the usual technique cannot be adopted.

Although TWSs to KSE do not continuously depend on c , our results show that TWSs to the filtered equation do. This fact reflects the breaking of the translational invariance by the filter. The details are discussed in the last part of this section. Thus the propagation velocity c becomes one of the control parameters of the solution and can be chosen arbitrarily in a certain range. See also schematic view in Fig.7.

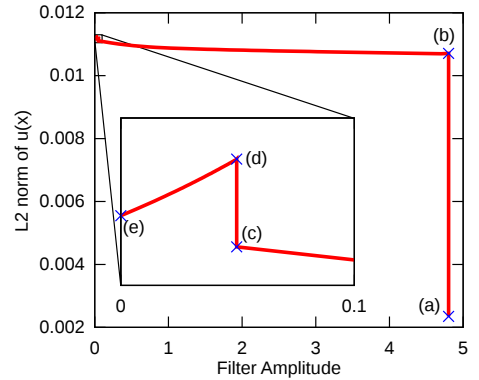


FIG. 8. (Color online) The trajectory of the continuation projected onto A_f - $\|u\|$ plane. A closeup around $A_f = 0$ is also shown.

Then the other issue arises; how do we obtain the specific value c_0 ? Although there is a range of c in which the solution exists continuously, this range becomes narrower and narrower as A_f goes to zero, and finally converges to a point on $A_f = 0$. We get over this issue by imposing an implicit relationship between c and A_f . This technique to impose the restriction is a key point to obtain a stream-wisely localized TWS. The details are discussed in the next subsection with our data.

B. Adopting the damping filtering method to KSE

In the first step of the damping filtering method, a localized region Ω is determined. We set the system size to $L = 200$ and the localized region $\Omega = [97, 103]$ in order to obtain a one-peak TWS. The filter function $H(x)$ is smoothed by Gaussian with $\sigma^2 = 0.01$ and the filter amplitude A_f is set to 4.8.

In the second step, a solution to the filtered Eq. (1) is obtained to start the continuation. As notated in the previous subsection, we can choose an arbitrary propagation velocity c in a certain range, and we choose $c = 0$ here. We execute a DNS of non-filtered equation (6) to produce a spatio-temporal chaotic field, which is used for an initial condition of a DNS of Eq. (6). This yields a stable solution, which is labeled as (a). These DNSs are solved by the quasi-spectral method with the classical forth-order Runge-Kutta method. Although a localized solution has an exponentially decaying tail and does not get exactly to zero in a finite distance, we regard small values comparable to the truncation error as zero and assume that the fixed boundary conditions $u(0) = u(L) = 0$ are satisfied. We use sine transform to ensure this condition with $N = 2048$ modes.

The third step is a continuation process. Since the propagation velocity c becomes a continuous parameter of the solution on $A_f > 0$ region, this continuation becomes essentially two-dimensional. It is almost impossible to obtain a full two-dimensional solution branch be-

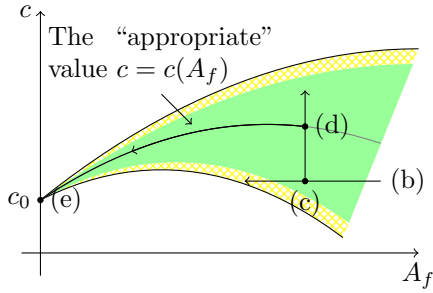


FIG. 9. (Color online) An schematic view of the parameter dependency of the solution around $A_f = 0$. The yellow (thin gray) crosshatched region denotes one where a solution continuously exists, and the green (thick gray) region denotes one where a “localized” solution continuously exists. Here a “localized” solution means that it does not have the oscillation around the boundary. The three steps are as follows: (i): (b) \rightarrow (c), (ii): (c) \rightarrow (d), (iii): (d) \rightarrow (e).

cause of the numerical cost, we introduce a path on A_f - c space as follows.

As noted above, if c is fixed to zero then a continuation with A_f yields the flat solution $u = 0$ before A_f reaches zero. In order to avoid this dead end, we first fix A_f to 4.8 and execute a continuation with c . The solution is traced up to $c \simeq 1.21$, which is labeled as (b). This value of c is determined by trial and error here, but a more practical criterion will be discussed in a future work.

The following continuation procedure is delicate because the uniqueness of the propagation velocity c must recover when $A_f = 0$. In short, the procedure consists of three steps (see Fig. 9): (i) A_f is reduced around 0.05 while c is fixed. (ii) A_f is fixed and c is adjusted to an “appropriate” value $c = c(A_f)$. (iii) c and A_f are traced simultaneously keeping the “appropriate” condition $c = c(A_f)$.

In the step (i), we fix c to 1.21 and execute a continuation with A_f . This continuation leads A_f around 0.01, but A_f cannot reach 0. In this continuation the profile of the solution changes as shown in Fig. 10. We define a characteristic length of the tail of the solution as the inverse of its decaying rate. As A_f decreases, it becomes longer and an oscillation starts to appear around the left boundary. If this tracing is continued further, the oscillation grows up and the solution may not be kept localized. Such non-localized solutions also cannot be traced till $A_f = 0$. This shows that a localized TWS to KSE cannot be obtained using only the continuation with A_f .

In order to avoid the oscillation around the boundary, we focus on the tail of the solution. In Fig. 10, the oscillation seems to appear when the tail loses its flat part. Indeed, at $A_f = 0.2244$ where its flat part is around $[0, 60]$ and $A_f = 0.1254$ where it is around $[0, 40]$ the oscillation does not appear. We conclude that the disappearance of the flat part, which may occur when $A_f < 1.0$, is a precursor of the oscillation at the boundary. We call this decrease of the flat part “the weakening

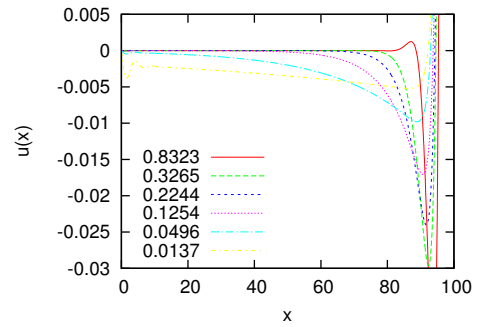


FIG. 10. (Color online) The left tails of the solutions obtained while the tracing (b) to (c) whose A_f is 0.8323, 0.3265, 0.2244, 0.1254, 0.0496 and 0.0137 respectively. As A_f decreases, the characteristic length of the tail becomes longer and longer. Finally an oscillation appears around the left boundary due to the boundary condition.

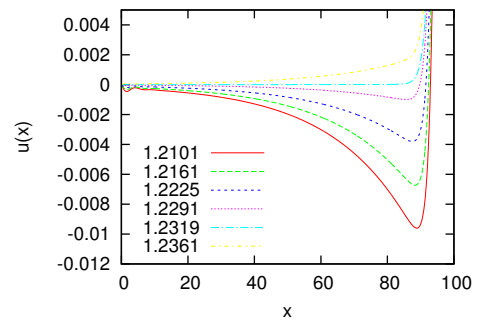


FIG. 11. (Color online) A part of the profile of solutions obtained while the tracing (c) \rightarrow (d) whose traveling velocity c is 1.2101(c), 1.2161, 1.2225, 1.2291, 1.2319(d), 1.2361. The mechanism of this weakening of the localization is argued in Section IV C.

of the localization”, and will discuss this mechanism in the next section.

We found that there exists a specific value c for each A_f such that the flat part recovers. Figure 11 shows the change in the tail of the solution while the continuation with c (A_f is fixed to 0.0496). At $c = 1.2319$ the flat part recovers to be $[0, 80]$. This continuation is the step (ii), and the “appropriate” value is $c = 1.2319$.

This “appropriate” value of c varies with A_f . In other words, the “appropriate” relation $c = c(A_f)$ defines a path on the two-dimensional parameter space c - A_f . Along this path the solution has always a flat part. In order to trace the solution along the path $c = c(A_f)$, however, it is necessary to express the condition $c = c(A_f)$ numerically. It can be easily done with the following integral value:

$$E_l = \int_0^l u(x) dx, \quad (7)$$

where l is chosen to be in the tail part. The change of E_l in the continuation mentioned above is shown in

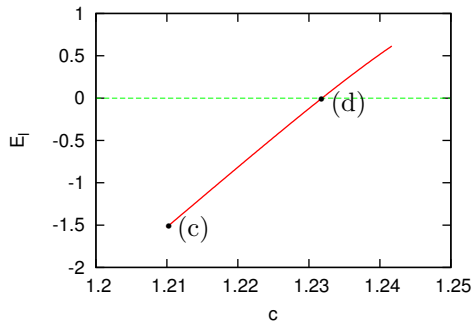


FIG. 12. (Color online) E_l is plotted against the traveling velocity c . E_l measures how long the tail of the solution is. $E_l(c)$ cross the line $E_l = 0$, and this point is labeled (d). This crossing behavior is also argued in Section IV C.

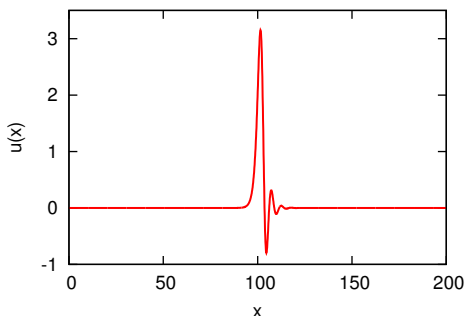


FIG. 13. (Color online) The profiles of TWS to Eq. (5). It takes non-zero value on a region $[90 : 115]$, which is much wider than $\Omega = [97 : 103]$.

Fig. 12. The relation $c = c(A_f)$ is now implicitly defined by $E_l(c, A_f) = 0$. Then we can continue the branch $u(x; c(A_f), A_f)$ with A_f . This conditional continuation can be implemented by a $(N + 1)$ -dimensional arc-length method, and we have succeeded to trace the solution till $A_f = 0$ within a numerical accuracy. This solutions is labeled as (e) in Fig. 8, and its profile is displayed in Fig. 13. Its propagation velocity $c_0 = c(0)$ equals to 1.2143. This is the same solitary-wave solution as that shown in fig.4c of [18].

C. Why the tail of the solution becomes longer?

In this subsection the mechanism of the weakening of the localization is considered. This weakening behavior enable us to obtain an implicitly defined path in A_f - c space. In order to generalize this technique to more complicated systems such as channel flows or pipe flows, it is necessary to investigate its details more precisely.

A steady localized solution $u(x)$ to Eq. (6) satisfies the ordinary differential equation:

$$\frac{d^4 u}{dx^4} + \frac{d^2 u}{dx^2} + (u - c) \frac{du}{dx} + A_f H(x) u = 0. \quad (8)$$

Here hats and primes are omitted for convenience. Regarding x as a virtual time, this equation defines a four-dimensional dynamical system. Then a localized solution $u(x)$ to Eq. (6) corresponds to a homoclinic orbit connecting the saddle point of this dynamical system, and the tails of the solution describes the asymptotic behavior of the homoclinic orbit from and to the saddle point. It should be noted that this reinterpretation has less compatibility with the fixed boundary condition $u(0) = u(L) = 0$ since we now consider the asymptotic behaviors in an infinite region $(-\infty, \infty)$ instead of the bounded region $[0, L]$. However the following arguments are all valid whenever $u(x)$ decays fast enough to be negligible comparing with the truncation error.

This dynamical system has a trivial fixed point (saddle point) $(u, \partial_x u, \partial_{xx} u, \partial_{xxx} u) = (0, 0, 0, 0)$ corresponding to the solution $u(x) = 0$ to Eq. (6). The localized solution $u(x)$ can be regarded as a homoclinic trajectory of this trivial fixed point. Then the tail of the localized solution can be analyzed by the eigenvalues of Jacobi matrix of this dynamical system at the fixed point. Since $H(x)$ equals to 1 in the tail region, the eigen equation of the Jacobi matrix becomes as follows:

$$\lambda^4 + \lambda^2 - c\lambda + A_f = 0. \quad (9)$$

This quartic equation has two real roots λ_0, λ_1 and two complex roots λ_{\pm} . Since we focus on the case $A_f \ll 1$, we first consider the case $A_f = 0$, and then a perturbation expansion about A_f .

When $A_f = 0$, the eigenvalues are $\lambda_0 = 0$ and three roots of a cubic equation $\lambda^3 + \lambda - c = 0$. This cubic equation has a real root λ_1 and two complex roots $\lambda_{\pm} = (-\lambda_1 \pm i\sqrt{3}\lambda_1^2 + 4)/2$. The real nonzero root λ_1 is positive when $c > 0$ and negative when $c < 0$, and here we consider the $c > 0$ case. Then the left and right tails of the solution can be written as follows:

$$u_L(x) = A_1 e^{\lambda_1 x}, \quad (10)$$

$$u_R(x) = A_+ e^{\lambda_+ x} + A_- e^{\lambda_- x}. \quad (11)$$

The coefficients A_1, A_+, A_- are determined in the nonlinear region. Since $\exp(\lambda_0 x)$ does not goes to zero as $x \rightarrow \pm\infty, u(x)$ cannot contain this term.

When $0 < A_f \ll 1$ the zero eigenvalue is modified as $\lambda_0 = A_f/c + O(A_f^2)$. Then the left tail of the solution can be written as follows:

$$u_L(x) = A_0 e^{\lambda_0 x} + A_1 e^{\lambda_1 x}. \quad (12)$$

The coefficients A_0 and A_1 are also determined in the nonlinear region, and depend both on c and A_f . Each of the terms in Eq. (12) defines a tail whose characteristic length is $1/\lambda_0$ and $1/\lambda_1$, and the realized tail is a superposition of them. As A_f goes to zero, the characteristic length $1/\lambda_0 = c/A_f$ diverges. Thus the modified eigenvalue λ_0 is the origin of the weakening, i.e., the long tail.

Next, we consider why we can obtain a solution with a short tail by the condition $E_l = 0$ for every small A_f . Using Eq. (12), E_l can be written as follows:

$$E_l \simeq \int_{-\infty}^l u_L(x) dx = \frac{A_0}{\lambda_0} e^{\lambda_0 l} + \frac{A_1}{\lambda_1} e^{\lambda_1 l}. \quad (13)$$

Since $1/\lambda_0 \gg 1/\lambda_1$ when $A_f \ll 1$, the first term in Eq. (12) is dominant except for a region near the nonlinear region. Thus the first term in Eq. (13) is rather dominant for an appropriate l . Then E_l roughly measures A_0 , and $E_l = 0$ is realized when A_0 is zero where the tail by λ_0 disappears. A more precise argument is also possible. The condition $E_l = 0$ can yield the condition of A_0 as follows:

$$\begin{aligned} A_0 &= -\frac{\lambda_0}{\lambda_1} A_1 e^{(\lambda_1 - \lambda_0)l} \\ &= -\frac{A_f}{c\lambda_1} A_1 e^{(\lambda_1 - \lambda_0)l} + O(A_f^2). \end{aligned} \quad (14)$$

Thus A_0 is not exactly zero while $A_f > 0$. However, since λ_0 goes to zero as $A_f \rightarrow 0$, A_0 satisfying this condition also goes to zero.

The essence of the above arguments is the existence of the zero eigenvalue λ_0 and its modification due to the damping. The modified zero eigenvalue introduces another degree of freedom in the determination of tails of solutions. Calculating the eigenvector of the zero eigenvalue, it corresponds to a uniform level raising of the velocity field, $u(x) \mapsto u(x) + \delta c$, so it corresponds to Galilean invariance. In other words, the reason why this small eigenvalue appears is the breakdown of Galilean invariance. This fact indicates that such the weakening of the localization is expected to occur whenever a stream-wisely localized TWS is going to be obtained in Galilean-invariant systems by our method.

At last, we conclude this section with an error estimate. Since the continuous parameter dependence on c disappears when $A_f = 0$, the continuation becomes unstable as A_f goes to zero. Although the point $A_f = 0$ is a singular point in this continuation problem, A_f can get an arbitrary value as small as the numerical accuracy allows. Indeed, we get $A_f \sim 10^{-10}$ in the conditional continuation. This is as small as a threshold for Newton method, $\varepsilon_{\text{Newton}}$. Then the continued solution can be regarded as a solution to KSE within an numerical error $\varepsilon_{\text{Newton}} + A_f \|u\|$.

V. CONCLUDING REMARKS

In this paper we introduce the damping filter method for obtaining spatially localized solutions. We adopt our method into two fundamental cases. First, in the Section III, we consider localized solutions to Swift-Hohenberg equation (SHE). Then our method can not only reproduce known solutions, but also obtain another spatially localized solution which belongs to a closed

isolated solution branch. Next, in the Section IV, we consider a stream-wisely localized traveling-wave solution (TWS) to Kuramoto-Sivashinsky equation (KSE). In this case, since the propagation velocity c is unknown, we have to continue the solution with c and the filter amplitude A_f . In order to make continuation one-dimensional we introduce an implicit condition about the tail of solutions. Here we reinterpret these result from a general point of view in order to adopt our method into more general cases.

The most interesting result in the Section III is the connection between two distinct solution branches. We show that two solution branches are connected with each other through the continuation with the filter amplitude A_f . We first introduce the filter term $-A_f H(x)u$ in order to obtain a guess at spatially localized solutions. However, it works as an excitation when $A_f < 0$. This excitation only works near the localized region where both $u(x)$ and $H(x)$ are non-zero. This causes an instability which may lead another localized solution. Indeed, we obtain the solution (d) in Section III only by the continuation with A_f . This spatially selective excitation mechanism has an advantage in searching spatially localized solutions. The result for SHE indicates that if another localized solution exists near the localized solution already obtained in the phase space, they may connect through this excitation mechanism. So our method may enable us to search localized solutions automatically.

In the Section IV, we have dealt with a spatially localized TWS to KSE. The main issue of this section is a treatment of the invariances. The damping filter term breaks the translational and Galilean invariances, but they recover when the filter disappears. This singular behavior is avoided by imposing the condition $c = c(A_f)$ by the implicit condition $E_l(c, A_f) = 0$.

This artificial condition can be reinterpreted as a critical line of the orbit-flip bifurcation [19]. For fixed A_f an orbit-flip bifurcation occurs when A_0 , defined in Section IV C, changes its sign with increasing c , see Fig. 9 and Fig. 11. Moreover, if $A_f \ll 1$, the relation $A_0 \sim A_f \sim 0$ holds on $c = c(A_f)$ because of Eq. (14). Therefore we can infer that the condition $c = c(A_f)$ corresponds to the critical line of the orbit-flip bifurcation in the four-dimensional ODE system Eq. (8).

To implement the critical condition directly, we can utilize an algorithm for tracking the orbit-flip bifurcation in AUTO [20]. This algorithm replaces the condition $E_l = 0$ with an orthogonal condition to keep the tangency between the homoclinic orbit and the leading eigenspace. Moreover, this method clarifies the mathematical meaning of our condition. However, since it is designed for a homoclinic orbit to ODE, it might be difficult to apply it for spatially two- or three-dimensional PDE systems. We thus expect that our method using E_l will be more suitable for the dynamical systems approach to turbulence.

ACKNOWLEDGMENTS

We thank T.Ogawa for invaluable comments on Swift-Hohenberg equation. We also appreciate the referee referring us to the orbit-flip bifurcation. This work was

supported by the Grants for Excellent Graduate Schools “The Next Generation of Physics, Spun from Universality and Emergence” from the Ministry of Education, Culture, Sports, Science, and Technology (MEXT) of Japan, and also partially by JSPS KAKENHI Grant Number 22540386. A part of numerical calculations were carried out on SR16000 at YITP in Kyoto University.

-
- [1] G. Kawahara, M. Uhlmann, and L. van Veen, *Annual Review of Fluid Mechanics* **44**, 203 (2012).
 - [2] J. Jiménez and P. Moin, *Journal of Fluid Mechanics* **225**, 213 (1991).
 - [3] T. Itano and S. Toh, *Journal of the Physical Society of Japan* **70**, 703 (2001).
 - [4] J. D. Skufca, J. A. Yorke, and B. Eckhardt, *Physical Review Letters* **96**, 174101 (2006).
 - [5] G. Kawahara and S. Kida, *Journal of Fluid Mechanics* **449**, 291 (2001).
 - [6] T. M. Schneider, B. Eckhardt, and J. A. Yorke, *Physical Review Letters* **99**, 034502 (2007).
 - [7] Y. Duguet, P. Schlatter, and D. S. Henningson, *Physics of Fluids* **21**, 111701 (2009).
 - [8] T. M. Schneider, D. Marinc, and B. Eckhardt, *Journal of Fluid Mechanics* **646**, 441 (2010).
 - [9] M. Avila, F. Mellibovsky, N. Roland, and B. Hof, *Physical Review Letters* **110**, 224502 (2013).
 - [10] J. Burke and E. Knobloch, *Chaos* **17**, 037102 (2007).
 - [11] E. Knobloch, *Nonlinearity* **21**, T45 (2008).
 - [12] M. Beck, J. Knobloch, D. J. B. Lloyd, B. Sandstede, and T. Wagenknecht, *SIAM Journal on Mathematical Analysis* **41**, 936 (2009).
 - [13] T. M. Schneider, J. F. Gibson, and J. Burke, *Physical Review Letters* **104**, 104501 (2010).
 - [14] A. Bergeon and E. Knobloch, *Physics of Fluids* **20**, 034102 (2008).
 - [15] M. Nagata, *Journal of Fluid Mechanics* **217**, 519 (1990).
 - [16] J. Jiménez and M. P. Simens, *Journal of Fluid Mechanics* **435**, 81 (2001).
 - [17] J. Knobloch, D. J. B. Lloyd, B. Sandstede, and T. Wagenknecht, *Journal of Dynamics and Differential Equations* **23**, 93 (2011).
 - [18] D. Michelson, *Physica D: Nonlinear Phenomena* **19**, 89 (1986).
 - [19] A. Champneys, Y. A. Kuznetsov, and B. Sandstede, *International Journal of Bifurcation and Chaos* **06**, 867 (1996).
 - [20] E. J. Doedel, R. C. Paffenroth, A. R. Champneys, T. F. Fairgrieve, Y. A. Kuznetsov, B. E. Oldeman, B. Sandstede, and X. J. Wang, <http://indy.cs.concordia.ca/auto/>.